

Calculating Properties of Exotic Hadrons Using Supervised Machine Learning

A Technical Report
presented to the faculty of the
School of Engineering and Applied Science
University of Virginia

by

Emma Yeats

May 10, 2021

On my honor as a University student, I have neither given nor received unauthorized aid on this assignment as defined by the Honor Guidelines for Thesis-Related Assignments.

Emma Yeats

Technical advisor: Dustin Keller, Department of Physics

Calculating Properties of Exotic Hadrons Using Supervised Machine Learning

Baryons and mesons are examples of ordinary hadrons, some of the most understood and precisely measured particles in nature. They are known to either exist as a quark-antiquark pair (meson) or as three valence quarks (baryon). However, it is speculated there are particles with a quark composition greater than three quarks, called exotic hadrons. These particles have incredibly short lifetimes and are difficult to predict, as we currently don't have a dependable method of estimating their location on the mass spectra line. In light of this dilemma, this research aims to use machine learning methods, along with the data we currently possess on ordinary hadrons, to predict characteristics of exotic hadron configurations and compare them with exotic candidates that have been found in experiment.

Background

Types of Exotics

An understanding of tetraquarks and pentaquarks is central to this research. Tetraquarks are composed of two quarks and two antiquarks, for a total of four elementary particles. Pentaquarks consist of three valence quarks and an additional quark-antiquark pair.

These exotic states share properties with ordinary hadrons, and fit into the baryon and meson subclasses. To classify as a baryon, a hadron must have an odd-numbered quark content, a $\frac{1}{2}$ -integer spin (baryons are fermions), and a "Baryon Number", B , equal to 1. Mesons, on the other hand, all have an even numbered quark content, whole integer spins (bosons), and $B = 0$.

Considering each quark is $B = \frac{1}{3}$, and each antiquark is $B = -\frac{1}{3}$, we can calculate Baryon Number using the following equation from [1],

$$B = \left(\frac{n_{quarks}}{3}\right) - \left(\frac{n_{antiquarks}}{3}\right). \quad (1)$$

If we were to calculate Baryon Number for an ordinary baryon using Equation (1), we see that $B = \frac{3}{3} - \frac{0}{3} = 1$. For an ordinary meson, we see $B = \frac{1}{3} - \frac{1}{3} = 0$. Similarly, we can also deduce that a pentaquark meets all conditions set to be classified as a baryon, and a tetraquark satisfies all conditions needed to classify as a meson.

There are exotics beyond these quark numbers, like the hexaquark. This hadron is expected to either be a dibaryon (six valence quarks) or made of three quark-antiquark pairs. The only known stable particle composed of purely six valence quarks is deuterium, a stable hydrogen isotope made of a proton and neutron [2]. Even so, this structure is not considered to be a dibaryon. While hexaquarks have not yet been detected or confirmed, as most accelerator experiments don't reach energies high enough to create them, they would likely be incredibly stable. Some have proposed them as a dark matter candidate, since they would decay so slowly their only interaction would be through gravity [3]. However, the fact that they have not been detected at all leaves them a poor candidate for this research's purposes.

There are other exotics also unstudied in this research that remain worth mentioning. The glueball, for instance, consists of purely gluons and no valence quarks. These are very difficult to identify as they mix with conventional mesons. They have not been observed with certainty, but should exist at energy range of current accelerators [4]. Additionally, hybrid mesons are likely excited gluons coupled to a conventional meson, and have been predicted by several models. These particles are expected to have different sets of quantum numbers, forbidden for conventional mesons by Quantum Chromodynamics [4].

Resonances

Each hadron configuration (for instance, uds , $\bar{u}s$ or $c\bar{c}d\bar{u}$) corresponds to a ground state particle and a collection of excited states, called resonances. The ground state particle has a longer lifetime and a smaller rest mass; the resonances decay quickly but have much larger rest masses. Resonances are typically specified by their masses, as there can be many of them for any particular quark composition. All ground state hadrons beyond the proton and neutron decay within a second, but resonances of hadron configurations decay faster as their energies increase. This is due to the strong interaction's dissipation at higher energies, resulting in an inability to stabilize the more massive and energetic particle [5][6][7].

Tools to Understand Quantum Chromodynamics

In Quantum Chromodynamics (QCD), the strength of the strong force is derived from coupling between quarks and gluons. This coupling becomes stronger at lower energies and leads to the diverse hadron spectrum of mesons and baryons physicists have detected today [7]. Studying the masses and widths of resonances and ground states for as many kinds of particles as possible can only aid in our understanding of the strong interaction [8]. Specifically, researching highly energetic resonances and exotic states will allow us to understand this fundamental force at higher energies, where it is least understood.

Currently, we can only estimate properties using the Lattice QCD Formalism, a powerful tool that is highly precise, yet incredibly laborious. Lattice calculations discretize general QCD onto a space-time lattice [9], which we can model using numerical methods. The recent advancement of computers and algorithms has allowed simulations to achieve much greater accuracy in recent years, with current Lattice simulations operating at the experimentally recorded quark masses.

However, the most advanced formalisms currently cannot account for isospin symmetry breaking, which leaves room for improvement [10].

Exotic Candidates

Exotic candidates have been detected at accelerator facilities around the world, beginning in the early 2000s. One of the first detections of an exotic state candidate was at KEK (Enerugi Kasokuki Kenkyū Kikō in Japan) by the Belle Collaboration in 2007. There, a $Z_c(4430)$ tetraquark was found in $B \rightarrow K \pi^\pm \psi'$ decays, with a quark content of $c\bar{c}d\bar{u}$ [11]. This particular particle was later confirmed by LHCb in 2014 [12].

Pentaquarks have been found at similar facilities. Namely, $P_c(4312)^+$, $P_c(4380)^+$, $P_c(4440)^+$, and $P_c(4457)^+$ were identified by LHCb in the $\Lambda_b^0 \rightarrow J/\psi K^- p$ decay chain [13]. Each of these particles were found to have a valence quark content of $uudc\bar{c}$ based on the constituents of the parent and sister particle in that decay step (Figure 1).

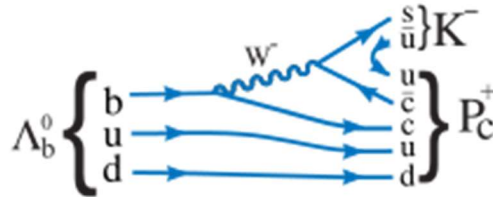


Figure 1: Feynman Diagram of $\Lambda_b^0 \rightarrow J/\psi K^- p$ Decay Step [13].

From the above Feynman diagram, one can also calculate the Isospin and Total Angular Momentum considering the meson K^- and baryon Λ_b^0 are measured with significance [1]. Parity may be more difficult to determine, since the above decay is a weak interaction where parity need not be conserved.

Figure 2, provided by LHCb [14], shows the experimental detection of these exotic states. The exotic state resonances are clearly shown in red, from which we can determine the exact mass of the resonance by comparing it with the background (shown as the black line in the figure). The deviations from the background are resonances, and deconstructed to determine the total rest mass of each in MeV (shown in color below the background line).

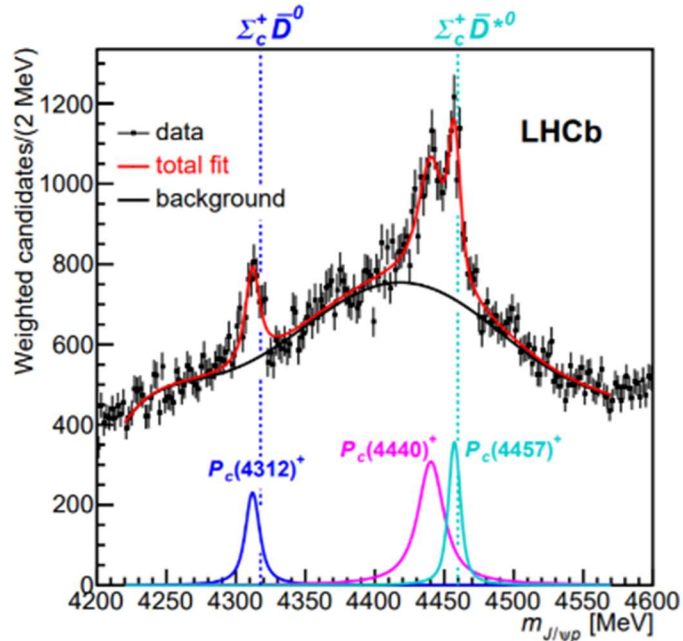


Figure 2: Pentaquark states discovered at LHCb [21].

Other exotic states have also been employed in the research. The $Z_c(3900)$ tetraquark was discovered independently in 2013 by the BES II detector at the Beijing Electron Positron Collider and the Belle Collaboration at KEK [15][16]. This exotic is recorded to have nearly all the same properties as $Z_c(4430)$, besides rest mass and width. Three other tetraquark candidates, $\chi(4274)$, $\chi(4500)$ and $\chi(4700)$, were found in July 2016 by LHCb [17][18]. All three were expected to have a quark content of $c\bar{c}d\bar{u}$, also making them charmonium tetraquarks.

Other exotic mesons like the π_1 group, the $f_0(500)$ and the $a_0(980)$, were initially considered. However, little is known definitively about these exotic mesons, and their quark

content remains largely unknown. The π_1 group in particular is still controversial, as it remains unclear if the structure is of a tetraquark or a hybrid meson [4][19]; thus, a specific quark content is difficult to determine with confidence.

Methodology

Machine Learning

The primary aim of this research is to provide an alternate method to the Lattice QCD formalism for the prediction of exotic mass ranges. Such predictions would help experimentalists “know where to look” for exotic hadrons.

Machine learning easily detect patterns within large datasets and can be used as a guide when determining where to search for exotic states. With quark content and quantum numbers as an input, a trained neural network will report its own theorized properties of particle configurations. These can then be compared to the reported experimental values.

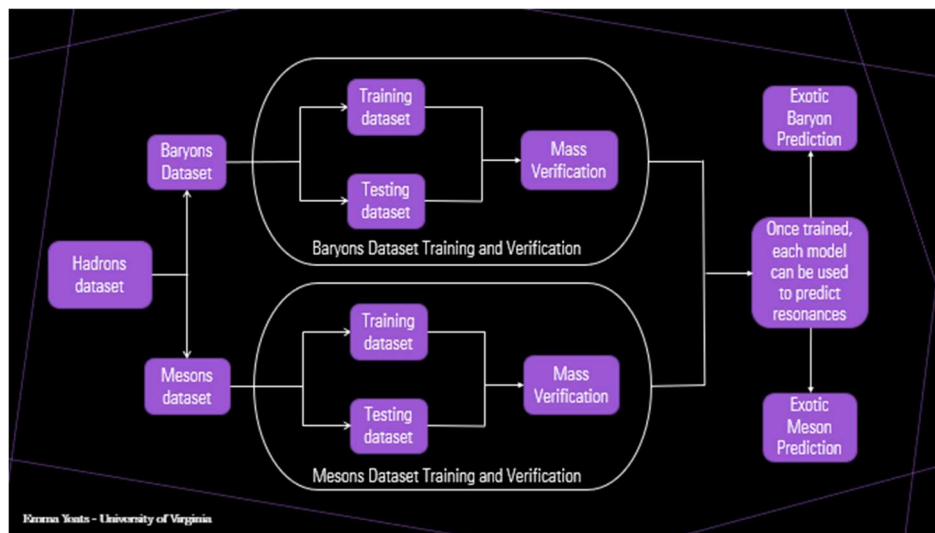


Figure 3: Neural Network Flowchart.

Figure 3 presents a map of the construction of the neural networks used for the experiment. The original hadrons dataset was split to create separate mesons and baryons datasets. Each one of those datasets was filtered and sorted to exclude null values before being split a second time into a “training dataset” and “testing dataset”. The training dataset is passed to the model, and is the only information the model uses while it learns.

Once the model is trained, we can then predict the testing dataset and compare the predictions with the reported experimental values. If predictions are consistent with the experimental values of the testing dataset, then the model has been verified to predict with some accuracy. Given this trained and verified model, predictions can be made on the properties of other (exotic) particles. Namely, we use the “meson model” to predict tetraquark properties, and the “baryon model” to predict pentaquark properties.

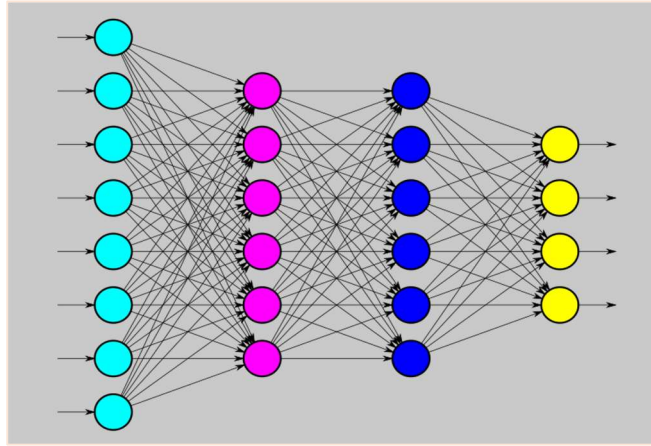


Figure 4: Sequential Model Construction [20].

For both datasets, a Sequential model type was chosen, which groups a “linear stack of layers” into a network [20], like the diagram shown in Figure 4. A layer is a callable object that takes one (or more) tensors as an input, transforms it, and outputs one (or more) tensors. The first

“layer” represents each individual feature from a given sample in the dataset. Each consecutive layer is “weighted” as the model learns. Every layer between the first and final layers are considered “hidden layers”, and the total number of layers can be changed by the programmer as a hyperparameter [20]. Each model can be finely tuned using other “hyperparameters” that influence its structure. These are the variables that change the model’s accuracy. For the baryon and meson models, the hyperparameters used are listed in Table I.

Table I: Hadron Models Hyperparameters

Parameter	Meson Model	Baryon Model
Model Type	Sequential	Sequential
1 st Layer	Dense, Units = 20, Activation Function = ‘elu’	Flatten
2 nd Layer	Dense, Units = 20, Activation Function = ‘elu’	Dense, Units = 18, Activation Function = ‘selu’
3 rd Layer	Dense, Units = 1	Dense, Units = 64, Activation Function = ‘selu’
4 th Layer	n/a	Dense, Units = 12, Activation Function = ‘selu’
5 th Layer	n/a	Dense, Units = 1
Loss Function	Mean Absolute Percentage Error	Mean Absolute Percentage Error
Optimizer, Learning Rate	FTRL, 0.4	Adadelata, 0.5
Epochs	1500	1500
Validation Split	0.2	0.1
Verbose	12	3

Collecting the Dataset

All data was collected from the Particle Data Group's (PDG) Website [21] from the Summary Tables and specific Particle Listings sections. The initial dataset contained 36 parameters for 500 ordinary hadrons, before being split up between baryons and mesons. 158 particles and 26 parameters were chosen for the meson dataset. The baryon dataset included 129 particles and 24 parameters, as this dataset excluded C and G Parity.

First, quark and antiquark content were included for all hadrons, and were taken directly from PDG or from [22][23] for $u, \bar{u}, d, \bar{d}, s, \bar{s}, c, \bar{c}, b$ and \bar{b} . The top and anti-top quarks were not included, as no trainable particles had these in their quark compositions. Quark content was typically represented by an integer value, except in mesons like π^0 , ω , or η' . For these mesons, quark content is expressed as a superposition – for instance, the η' quark content is expressed as,

$$\frac{1}{\sqrt{3}}(u\bar{u} + d\bar{d} + s\bar{s}). \quad (2)$$

These mesons required the content of the $u, \bar{u}, d, \bar{d}, s$ and \bar{s} parameters to each be $\sqrt{\frac{1}{3}}$.

Some mesons, like the π^0 , had a quark content that included a negative contribution, shown in the following expression;

$$\frac{1}{\sqrt{2}}(u\bar{u} - d\bar{d}). \quad (3)$$

Mesons with similar quark contents were not included in the meson dataset due to the negative contribution of $\frac{1}{\sqrt{2}}d\bar{d}$. This requires a complex value to fully define.

All reported masses and mass errors were included as parameters in both datasets, in MeV/c^2 . Since this became the predicted parameter, and these models required verification, particles that did not include a rest mass measurement were excluded from the dataset. Charge (Q) and Baryon

Number (B) were included as well, and while the formula for B is given in Equation (1), charge is given by:

$$Q = \frac{2}{3}(n_u - n_{\bar{u}}) - \frac{1}{3}(n_d - n_{\bar{d}}) + \frac{2}{3}(n_c - n_{\bar{c}}) - \frac{1}{3}(n_s - n_{\bar{s}}) - \frac{1}{3}(n_b - n_{\bar{b}}) + \frac{2}{3}(n_t - n_{\bar{t}}). \quad (4)$$

...where $(n_u - n_{\bar{u}})$ is the number of up antiquarks subtracted from the number of up quarks for that particle. For all particles in the datasets, the top quark contribution was zero, so Equation (4) reduces to,

$$Q = \frac{2}{3}(n_u - n_{\bar{u}}) - \frac{1}{3}(n_d - n_{\bar{d}}) + \frac{2}{3}(n_c - n_{\bar{c}}) - \frac{1}{3}(n_s - n_{\bar{s}}) - \frac{1}{3}(n_b - n_{\bar{b}}). \quad (5)$$

Lifetime (τ) or width (Γ) was also reported for each hadron. To understand this parameter, one must investigate the properties of ground state particles and their resonances. Ground state hadrons are only classified by lifetimes. Resonances are reported by their widths, which are fairly large and can be converted into lifetime using the relation,

$$\Gamma = \frac{\hbar}{\tau} \quad (6)$$

...where $\hbar = \frac{h}{2\pi}$, and h is Planck's constant. Lifetime is measured in seconds, and is the elapsed time the particle is observed to exist. Width is a direct result of the Uncertainty Principle,

$$\Delta E \Delta t > \frac{\hbar}{2} \quad (7)$$

...where ΔE is the uncertainty in mass energy, and is taken to be $\Gamma/2$ [24]. Thus, width is measured in MeV.

There were properties used to review each particle: Charm (C), Strangeness (S), Bottomness (B') and Topness (T). Topness is zero for all particles used in training; the other values were calculated using the following:

$$C = n_c - n_{\bar{c}} \quad (8)$$

$$S = -(n_s - n_{\bar{s}}) \quad (9)$$

$$B' = -(n_b - n_{\bar{b}}) \quad (10)$$

The variables above appear when calculating quantum numbers, the inclusion of which heavily increased prediction accuracy. Isospin (I), Total Angular Momentum (J) and Parity (P) were included as parameters for both the mesons and baryons models. C Parity (C) and G Parity (G) are only defined for mesons, and it was decided that only mesons with both of these quantum numbers known would be included. Three more quantum numbers were not recorded by PDG, and instead calculated using quark content. I_3 , the 3rd component of isospin [25], is only nonzero for up and down quarks. It is represented by,

$$I_3 = \frac{1}{2}(n_u - n_{\bar{u}} - n_d + n_{\bar{d}}). \quad (11)$$

Weak isospin, T_3 , is given by:

$$T_3 = \frac{1}{2}[(n_u - n_{\bar{u}}) - (n_d - n_{\bar{d}}) + (n_c - n_{\bar{c}}) - (n_s - n_{\bar{s}}) - (n_b - n_{\bar{b}})]. \quad (12)$$

And hypercharge, Y , is expressed as,

$$Y = B + S + C + B' + T' = B + S + C + B' \quad (T = \text{Topness} = 0) \quad (13)$$

Above, B is Baryon Number as given in Equation (1), S is Strangeness given in Equation (9), C is Charm from Equation (8), and B' is Bottomness as seen in Equation (10).

Results

After ideal hyperparameters were determined, the meson and baryon models were trained 20 times independently. Each independent training session then generated its own prediction of the testing dataset, giving 20 separate predictions on the same hadron. The full range of predictions was determined from this and classified as the model error. The model predictions were then compared with experimental observations and Lattice QCD (LQCD) predictions.

Baryons Training

Four ordinary baryons were chosen for the baryon model testing. Initially, the model used the baryons $N(1710)\frac{1}{2}^+$ and $\Xi_c(2815)^+$ as testing parameters, to validate the model's mass predictions. Those predictions are plotted and compared with experimental observations and LQCD predictions [26][27][28] in Fig. 5, and organized by Total Angular Momentum.

To study the model further, two baryons originally placed in the training dataset, $\Lambda_c(2625)$ and $\Delta(1600)\frac{3}{2}^+$, were swapped with the initial testing dataset. The model's predictions on those particles are displayed similarly in Fig. 6, with LQCD predictions from [26][27], and are shown with the true error of the model calculated over the 20 training sessions. The predictions in the figures are within 300 MeV of experimental ranges.

A noticeable outlier is $\Delta(1600)\frac{3}{2}^+$, which was not precisely predicted by the model (although also not predicted by LQCD). Otherwise, the other ranges of predictions span or meet the experimentally recorded values of the baryons.

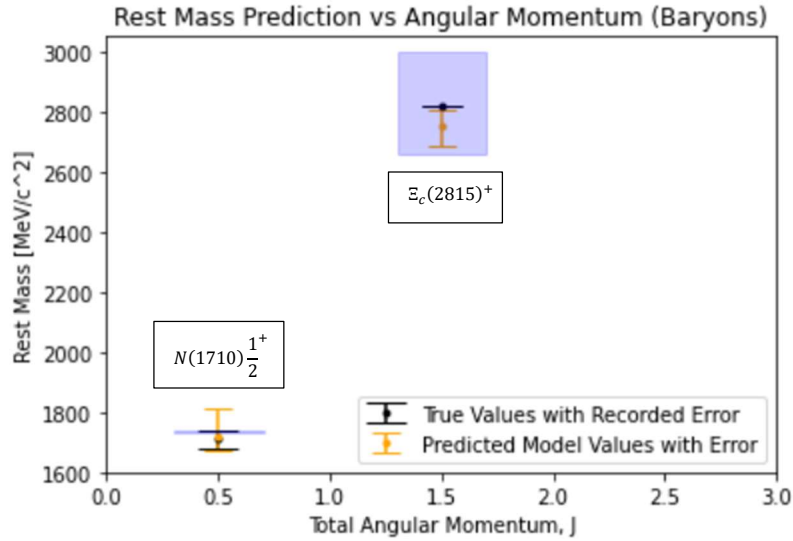


Figure 5. $N(1710)_{\frac{1}{2}}^{1+}$ and $E_c(2815)^+$ mass predictions in MeV/c^2 shown with model error in orange error bars. They are compared with experimental ranges for each, in black error bars, and Lattice QCD predictions in the blue shaded regions [26][27][28]. Organized by Total Angular Momentum, J.

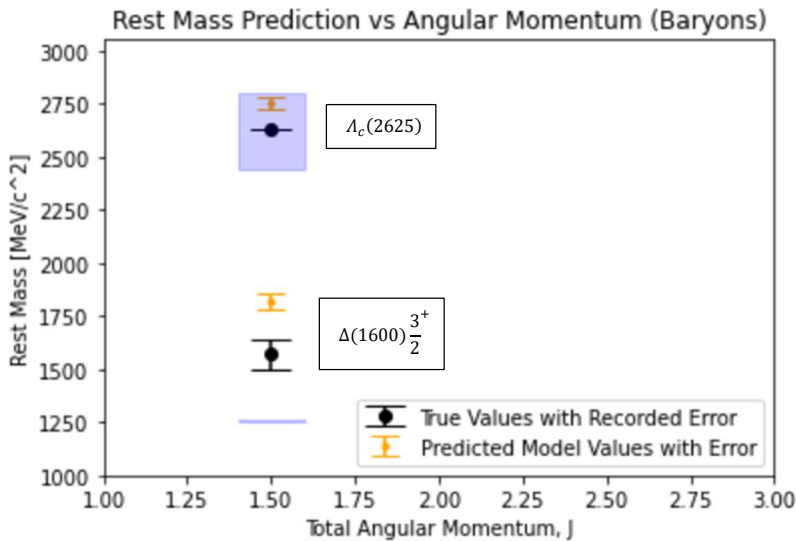


Figure 6. $\Lambda_c(2625)$ and $\Delta(1600)_{\frac{3}{2}}^{3+}$ mass predictions in MeV/c^2 shown with model error in orange error bars. They are compared with experimental ranges for each, in black error bars, and Lattice QCD predictions in the blue shaded regions [26][27]. Organized by Total Angular Momentum, J.

Mesons Training

The mesons model was trained and tuned using the hyperparameters shown in the second column of Table I. Following the same testing methodology as the baryon model, the meson model was first tested with the ordinary mesons $D^*(S2)(2573)^-$ and $\chi(B1)(2P)$. The results of those predictions are shown in Fig. 7. These were then exchanged with the ρ^+ and B_c^+ mesons (Fig. 8). LQCD predictions for these mesons were collected from [26][29][30][31].

Like the tested baryons, three of the mesons were predicted within error. B_c^+ , a bottomonium meson, was not predicted by the model. It remains nearly 800 MeV away from the accurate value. The lower prediction accuracy and higher model error likely results from the large range of masses predicted over; thus, the meson model requires finer hyperparameter tuning. Achieving optimal tuning is a main component of ensuring consistency between particle prediction accuracies.

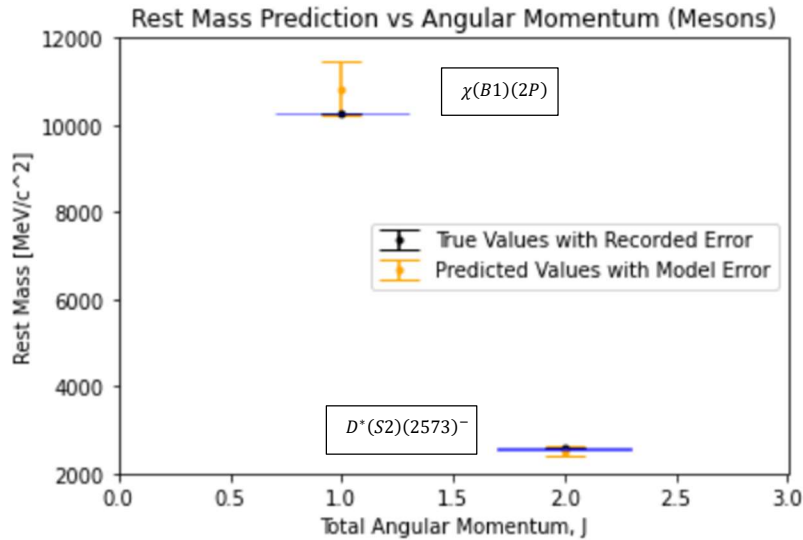


Figure 7. $D^*(S2)(2573)^-$ and $\chi(B1)(2P)$ mass predictions in MeV/c^2 shown with model error in orange error bars. They are compared with experimental ranges for each, in black error bars, and Lattice QCD predictions in the blue shaded regions [30][31]. Organized by Total Angular Momentum, J.

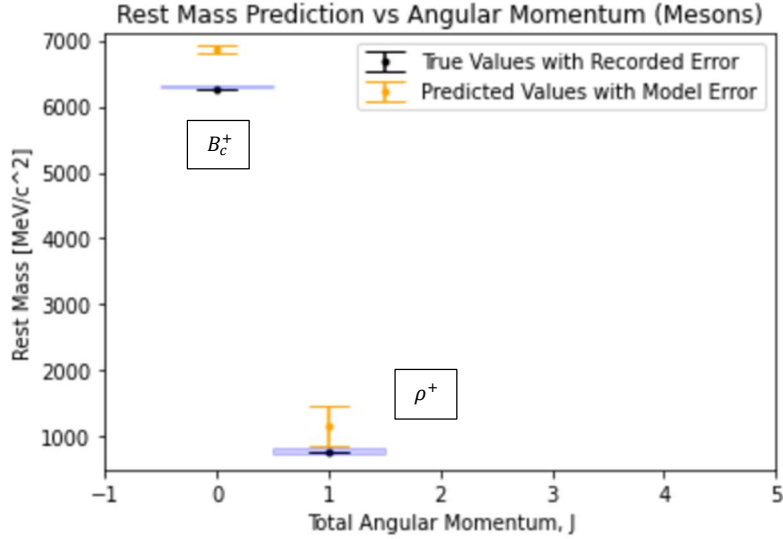


Figure 8. ρ^+ and B_c^+ mass predictions in MeV/c^2 shown with model error in orange error bars. They are compared with experimental ranges for each, in black error bars, and Lattice QCD predictions in the blue shaded regions [26][29]. Organized by Total Angular Momentum, J.

Comparison with Experiment

Figures 9 and 10 showcase the predictions made on exotic states, and are arranged in similar formats to those shown previously. Exotics meson predictions are shown in Figure 9, and exotic baryons in Figure 10. Specifically, predictions for the tetraquarks $Z_c(4430)$, $Z_c(3900)$, $\chi_{c1}(4274)$, $\chi_{c0}(4500)$ and $\chi_{c0}(4700)$ are compared with the experimentally measured masses for each, as well as the LQCD predictions for $Z_c(4430)$ and $\chi_{c1}(4274)$ from [32][33]. The three other states have not been predicted as of yet [33]. As seen in the figure, the meson model predicted just below the experimentally recorded range of the Z_c tetraquark group. Although the prediction error is very high, the maximum of the range resulted in fairly accurate predictions for the χ_{c1}, χ_{c0} group.

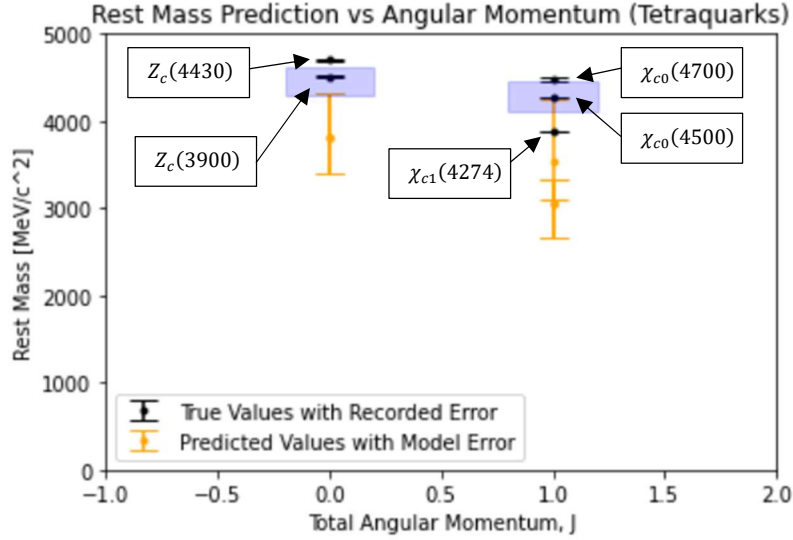


Figure 9. Tetraquark mass predictions in MeV/c^2 shown with model error in orange error bars. They are compared with experimental ranges for each, in black error bars, and Lattice QCD predictions in the blue shaded regions [32][33]. Organized by Total Angular Momentum, J.

The pentaquarks $P_c(4312)^+$, $P_c(4380)^+$, $P_c(4440)^+$ and $P_c(4457)^+$ were chosen to test the baryons model. Predictions for these exotics are compared with their experimental values in Figure 10, and shown with the LQCD predictions for all particles but $P_c(4457)^+$, as this resonance has no recorded LQCD prediction [34]. The pentaquarks have the same quark composition and quantum numbers. Thus, as there were no distinguishing parameters, all four were predicted at the same mass by the model.

These particular predictions are far from the observed values. During the tuning stage of this research, very few changes could be made to this prediction accuracy even as hyperparameters and model accuracy varied wildly. In the future, an optimization of hyperparameters may assist in increasing the accuracy of the baryon model in pentaquark prediction.

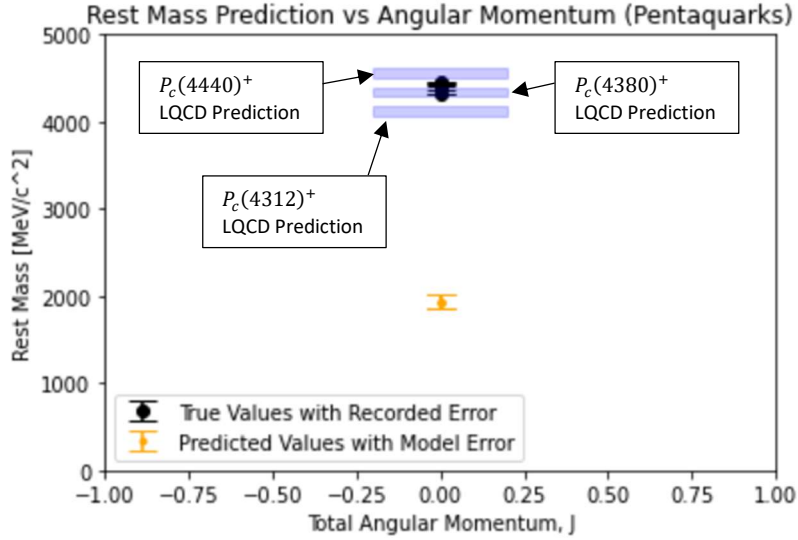


Figure 10. Pentaquarks mass predictions in MeV/c^2 shown with model error in orange error bars. They are compared with experimental ranges for each, in black error bars, and Lattice QCD predictions in the blue shaded regions [34]. Organized by Total Angular Momentum, J .

Future Work

There are several ways in which this research can be improved or expanded on in the future. Improving the mesons and baryons models themselves can be done by creating an optimization code to more accurately identify the best hyperparameters. Further splitting the datasets to study resonances and ground state particles separately may also improve prediction, but would likely not include enough datapoints to produce an accurate model. Real and imaginary pole position may also be included as parameters in the future [35], although the sparsity of reporting of these values will require a change in how the algorithms first sorts through null values.

Beyond these changes, the most important will be in obtaining as many trainable particles as possible to include in the datasets. Thus, adding more particles to either dataset will increase prediction accuracy on future simulations. This requires the inclusion of more particles with superpositions for quark content, like in Equation (3), and gathering more information on quantum numbers and widths to decrease the number of null values.

One of the original goals of this research was to additionally make predictions on the lifetimes of exotic states from their masses. However, lifetime is a very small quantity, as all known hadrons but the proton and neutron have lifetimes below 10^{-7} seconds. The parameter varies from 10^{37} to 10^{-2} seconds over the total hadrons dataset. While an attempt was made to create a lifetime prediction model, floating point errors surfaced due to the nature of the data and made prediction-making difficult. A model for width prediction was also created, but currently includes too few trainable datapoints to create a viable model (less than 100 trainable baryons). Thus, lifetime and width were left out entirely. Changing the algorithm to include width and lifetime predictions in the future is a top priority and would be helpful in the search for exotics.

A final task is determining the commonality between particles that the baryons and mesons models were able to predict well. An analysis on the similarities and differences in quantum numbers, quark content and energy is instrumental to crafting a better understanding of where (and why) the model is successful.

Conclusion

Both the baryons and mesons models were able to predict several particles well, and predict all ordinary hadrons within 1000 MeV. The meson model in particular shows additional promise in mass prediction of tetraquarks. Additionally, that the mesons model was able to predict exotic states more precisely than the baryons model, despite the model itself having a greater general error in predicting ordinary mesons, is of great interest. While improvements in both models are necessary to have more faith in their predicting power, the successes that have been reached in these early stages of development are encouraging for the method as a whole.

References

- [1] Griffiths, D. (2014). Introduction to Elementary Particles. *Wiley-VCH Publishing*. Second, Revised Edition. 8th Reprint.
- [2] Arnoux, R. (2011). Deuterium: A Precious Gift From the Big Bang. *Iter Newslines*. <https://www.iter.org/newslines/167/631>
- [3] Sutter, P. (2020). Oddball sexaquark particles could be immortal, if they exist at all. *Live Science Online*. <https://www.livescience.com/sexquarks-could-explain-dark-matter.html>
- [4] Somov, A. (2016). Hall D / GlueX Physics Program. *The 8th Workshop on Hadron Physics in China and Opportunities Worldwide, Wuhan, China, 8 – 11 August 2016*.
- [5] Ceci, S., Hadžimehmedović, M., Osmanović, H., Percan, A. & Zauner, B. (2017). Fundamental properties of resonances. *Nature Scientific Reports*. <https://www.nature.com/articles/srep45246>
- [6] Dalitz, R.H. & Moorhouse, R.G. (1970). What is resonance? *The Royal Society Publishing*. doi.org/10.1098/rspa.1970.0145
- [7] The GlueX Collaboration. (2010). The GlueX Experiment in Hall-D. www.gluex.org/docs/pac36_update.pdf
- [8] Olsen, S.L. (2014). A new hadron spectroscopy. *Front. Phys.* 10, 101401 (2015). doi.org/10.1007/S11467-014-0449-6
- [9] Davies, C. (2005). Lattice QCD – A guide for people who want results. *arXiv*. <https://cds.cern.ch/record/884217/files/0509046.pdf>
- [10] M. Tanabashi et al. (Particle Data Group). (2019). *Phys. Rev. D* 98, 030001 (2018) December 6, 2019 11:49am
- [11] Belle Collaboration: S.-K. Choi, S.L. Olsen, et al. (2008). *Physical Review Letters* 100:142001, 2008. [arXiv:0708.1790](https://arxiv.org/abs/0708.1790) [hep-ex]
- [12] LHCb Collaboration. (2014). *Physical Review Letters* 112, 222002 (2014). [arXiv:1404.1903](https://arxiv.org/abs/1404.1903) [hep-ex]
- [13] R. Aaij et al. (LHCb collaboration). (2015). Observation of J/ψ resonances consistent with pentaquark states in $\Lambda_b^0 \rightarrow J/\psi K^- p$ decays. *Physical Review Letters*. 115 (7): 072001. [arXiv:1507.03414](https://arxiv.org/abs/1507.03414)
- [14] P.A. Zyla et al. (Particle Data Group). (2020). *Progress of Theoretical and Experimental Physics*. 2020, 083C01. 2020. June 1, 2020 8:31am

- [15] Ablikim, M.; BESIII Collaboration; et al. (2013). Observation of a Charged Charmoniumlike Structure in $e^+e^- \rightarrow \pi^+\pi^-J/\psi$ at $\sqrt{s} = 4.26$ GeV. *Physical Review Letters*. 110 (25): 252001. [arXiv:1303.5949](https://arxiv.org/abs/1303.5949)
- [16] Xiao, T., Dobbs, S., Tomaradze, A. & Seth, K. K. (2013). Observation of the Charged Hadron $Z_c^\pm(3900)$ and Evidence of the Neutral $Z_c^0(3900)$ at $\sqrt{s} = 4170$ MeV. *Physics Letters B*. 727: 366–370. [arXiv:1304.3036](https://arxiv.org/abs/1304.3036)
- [17] R. Aaij; et al. (LHCb collaboration). (2017). Observation of $J/\psi\phi$ structures consistent with exotic states from amplitude analysis of $B^+ \rightarrow J/\psi\phi K^+$ decays. *Physical Review Letters*. 118 (2): 022003. [arXiv:1606.07895](https://arxiv.org/abs/1606.07895)
- [18] R. Aaij; et al. (LHCb collaboration). (2017). Amplitude analysis of $B^+ \rightarrow J/\psi\phi K^+$ decays. *Physical Review D*. 95 (1): 012002. [arXiv:1606.07898](https://arxiv.org/abs/1606.07898)
- [19] M. Tanabashi et al. (Particle Data Group). (2018). *Phys. Rev. D* 98, 030001 (2018) June 5, 2018 20:07
- [20] Layers In A Neural Network Explained – Machine Learning & Deep Learning Fundamentals. 2017. Deeplizard. <https://deeplizard.com/learn/video/FK77zZxaBoI>
- [21] P.A. Zyla et al. (Particle Data Group). (2020). *Progress of Theoretical and Experimental Physics*. 2020, 083C01 (2020).
- [22] Nave, R. (2017). Mesons. *Hyperphysics*. <http://hyperphysics.gsu.edu/hbase/Particles/meson.html>
- [23] Nave, R. (2017). Table of Baryons. *Hyperphysics*. <http://hyperphysics.gsu.edu/hbase/Particles/baryon.html#c1>
- [24] Nave, R. (2017). Particle lifetimes from the uncertainty principle. *Hyperphysics*. <http://hyperphysics.phy-astr.gsu.edu/hbase/quantum/parlif.html>
- [25] Martin, V. (2012). Lecture 11: Mesons and Baryons. Particle Physics, Spring Semester 2012. https://www2.ph.ed.ac.uk/~vjm/Lectures/SHParticlePhysics2012_files/PPLecture11.pdf
- [26] Klempt, E. & Richard, J. (2009). Baryon Spectroscopy. *Review for Modern Physics*. [arXiv:0901.2055](https://arxiv.org/abs/0901.2055) [hep-ph]
- [27] Wang, Z. G. (2015). Analysis of the $\chi_c(2625)$ and $\chi_c(2815)$ with QCD sum rules. *arXiv*. [arXiv:1503.06740](https://arxiv.org/abs/1503.06740) [hep-ph]
- [28] Abe, K. et al. (The Belle Collaboration). (2006). Measurement of masses of $\Xi_c(2645)$ and $\Xi_c(2815)$ baryons. *arXiv*. [arXiv:hep-ex/0608012](https://arxiv.org/abs/hep-ex/0608012)

- [29] Davies, C. (2006). Precision lattice QCD calculations and predictions of fundamental physics in heavy quark systems. *Journal of Physics: Conf. Ser.* 46 016
- [30] Bartelt, J. & Shukla, S. (1995). Charmed Meson Spectroscopy. *Annual Review of Nuclear and Particle Science*, 45:133-61.
- [31] Liu, J. F. & Ding, G. J. (2011). Bottomonium Spectrum with Coupled-Channel Effects. *European Physical Journal C*. [doi: 10.1140/epjc/s10052-012-1981-6](https://doi.org/10.1140/epjc/s10052-012-1981-6)
- [32] Prelovsek, S. et al. (2015). Study of the $Z + c$ channel using lattice QCD. *Physical Review D*. [arXiv:1405.7623](https://arxiv.org/abs/1405.7623) [hep-lat]
- [33] Prelovsek, S. (2019). Lattice spectroscopy (focus on exotics). Proceedings of Science. [arXiv:2001.01767v2](https://arxiv.org/abs/2001.01767v2) [hep-lat]
- [34] Skerbis, U. & Prelovsek, S. (2019). Nucleon- J/ψ and nucleon- η_c scattering in Pc pentaquark channels from LQCD. *Physical Review D*. [arXiv:1811.02285v3](https://arxiv.org/abs/1811.02285v3) [hep-lat]
- [35] Ceci, S., Hadžimehmedović, M., Osmanović, H., Percan, A. & Zauner, B. (2017). Fundamental properties of resonances. *Nature Scientific Reports*. <https://www.nature.com/articles/srep45246>